Original Article

Proteomics Study of Benzene Metabolite Hydroquinone Induced Hematotoxicity in K562 Cells*

JIN Yi Shan[1,&], YI Zong Chun[1,&], ZHANG Yu Jing[1], RONG Long[1], and YU Chun Hong[2,#]

1. School of Biological Science and Medical Engineering, Beihang University, Beijing 100191, China; 2. School of Engineering Medicine, Beihang University, Beijing 100191, China

Abstract

Objective Hydroquinone (HQ), one of the phenolic metabolites of benzene, is widely recognized as an important participant in benzene-induced hematotoxicity. However, there are few relevant proteomics in HQ-induced hematotoxicity and the mechanism hasn't been fully understood yet.

Methods In this study, we treated K562 cells with 40 μmol/L HQ for 72 h, examined and validated protein expression changes by Label-free proteomic analysis and Parallel reaction monitoring (PRM), and performed bioinformatics analysis to identify interaction networks.

Results One hundred and eighty-seven upregulated differentially expressed proteins (DEPs) and 279 downregulated DEPs were identified in HQ-exposed K562 cells, which were involved in neutrophil-mediated immunity, blood microparticle, and other GO terms, as well as the lysosome, metabolic, cell cycle, and cellular senescence-related pathways. Focusing on the 23 DEGs and 5 DEPs in erythroid differentiation-related pathways, we constructed the network of protein interactions and determined 6 DEPs (STAT1, STAT3, CASP3, KIT, STAT5B, and VEGFA) as main hub proteins with the most interactions, among which STATs made a central impact and may be potential biomarkers of HQ-induced hematotoxicity.

Conclusion Our work reinforced the use of proteomics and bioinformatic approaches to advance knowledge on molecular mechanisms of HQ-induced hematotoxicity at the protein level and provide a valuable basis for further clarification.

Key words: Hydroquinone; Proteomics; Hematotoxicity; K562 cells

Biomed Environ Sci, 2024; 37(4): 341-353 doi: 10.3967/bes2024.039 ISSN: 0895-3988

www.besjournal.com (full text) CN: 11-2816/Q

INTRODUCTION

Benzene is a widely recognized environmental pollutant that chronic exposure can induce hematotoxicity, augmenting the risk of aplastic anemia and hematological neoplasms, especially in occupationally exposed populations[1,2]. After entering the body, benzene is metabolized in the liver, lung, and bone marrow, transforming into various metabolites including phenol and hydroquinone (HQ), while an increasing number of studies have demonstrated the pivotal role of these phenolic metabolites in the benzene-induced hematotoxicity[3-9].

Among these metabolites, HQ is a major active metabolite and often serves as a substitute for benzene *in vitro* experiments. Our previous study

*This study was supported by the National Natural Science Foundation of China [Project No.81573192].

&These authors contributed equally to this work.

#Correspondence should be addressed to YU Chun Hong, Lecturer, PhD, Tel: 86-10-82313117, E-mail: chunhongyu@buaa.edu.cn

Biographical notes of the first authors: JIN Yi Shan, female, born in 2002, Undergraduate, majoring in biomedical engineering; YI Zong Chun, male, born in 1971, PhD, Associate Professor, majoring in cellular and molecular toxicology.

identified that, during hemin-induced erythroid differentiation, HQ distinctly inhibited the expression of globin genes and critical transcription factor genes (GATA-1 and NF-E2)[7], while transcription of some erythroid-related genes was down-regulated by HQ-induced DNA methylation[10,11]. Other epigenetic changes, including histone modifications, aberrant expression of ncRNAs, and chromatin remodeling, also involve in HQ-induced hematotoxicity[12,13]. It has been reported that HQ induced the generation of reactive oxygen species (ROS), the phosphorylation of histone γ-H2AX, and the production of the DNA damage-responsive enzyme PARP-1, consequently leading to cell apoptosis *via* a mitochondria-mediated apoptotic pathway in TK6 cells[14]. Consistently, we have proved that exposure to HQ induced increases in ROS, the activity of caspase-8, the expression of Fas and FasL on the cell surface, and the decrease in the cell surface sialic acid level, which not only affected cell cycles but induced the inhibition of erythroid differentiation and apoptosis as well in K562 cells[15,16]. Recent studies focused on the effects of microRNAs (miRNAs) expression changes in HQ-induced hemotoxicity and leukemogenesis[9,17,18]. Some researchers have proposed that the down-regulation of miRNA-451a and miRNA-486-5p might involve in HQ-induced inhibition of erythroid cell differentiation in $CD34^+$ hematopoietic progenitor cells[9], besides miR-1246 and miR-224 were the potential major regulators in HQ-exposed K562 cells[18].

Proteomics aims to identify and quantify the compositions, expression levels, post-translational modification, interactions, and functions in tissues and cells of all proteins in a given sample[19,20]. Proteins are the final product of gene expression and directly regulate the life activities of organisms. Applying proteomics to environmental toxicology research is conducive to identifying and screening new high-sensitivity protein markers, which will contribute to revealing the toxicological molecular mechanism of exogenous substances more intuitively and deeply[21-23]. Reports on the toxicological mechanism of hematotoxicity of benzene and HQ mostly focus on genomics and transcriptomic analysis[9,17,18,24-26], especially the analysis of miRNA expression[9,17,18,25]. However, there are few relevant reports on proteomic analysis. Although these studies have clarified some important potential mechanisms of benzene and HQ-induced hematotoxicity, they are not as intuitive as proteomic analysis of the final product protein of gene expression and may omit information leading to incomplete analysis.

Based on previous studies, we hypothesized that HQ mainly induces hematotoxicity by inhibiting hematopoietic differentiation, especially erythroid differentiation. Human leukemia K562 cells were derived from a patient with chronic myeloid leukemia and can be induced to red cell differentiation *in vitro*, which can be served as a good model system for investigating erythroid differentiation[27,28]. Therefore, through label-free proteomic analysis and bioinformatics methods, this study aims to screen HQ-induced differentially expressed proteins (DEPs) in K562 cells and identify their functions and signaling pathways involved in regulation and the networks of protein interactions, especially in erythroid differentiation, so that we can have a deeper understanding of the mechanism of HQ-induced hemotoxicity.

MATERIALS AND METHODS

Cell Culture

Human leukemia K562 cells were purchased from Cell Resource Center, Peking Union Medical College (CRC/PUMC, China), and were cultured in RPMI-1640 culture medium (Invitrogen) supplemented with 10% (V/V) fetal bovine serum (FBS) (HyClone), 100 U/mL penicillin (Sigma-Aldrich), and 100 μg/mL streptomycin (Sigma-Aldrich) in a humidified 5% CO_2 incubator at 37 °C. Exponentially growing K562 cells at passages 4–8 after recovery were collected and re-suspended in a fresh culture medium. According to our previous study[7], after K562 cells were treated with 40 μmol/L HQ (Sigma-Aldrich) for 72 h, the cells were harvested for further study.

Label-free Proteomic Analysis

Mass spectrometry (MS) analyses were performed at the Peking University medical and health analytical center using 200 μg protein samples. The protein samples were denatured using 8 mol/L urea, diluted using 10 mmol/L dithiothreitol (DTT), alkylated using 1 mol/L iodoacetamide, washed three times with 50 mmol/L ammonium bicarbonate and digested with trypsin at 37 °C overnight. The digestion was quenched with 50 mmol/L ammonium bicarbonate and dried in a vacuum concentrator.

The desalted peptides were separated by high-pH reversed-phase high-performance liquid chromatography (RP-HPLC). The samples were dissolved in mobile phase A (20 mmol/L ammonium formate, pH = 10), mixed well by vortex shock, and centrifuged at 12,000 ×*g* for 20 min. The supernatants were desalted on the C18 precolumn (3.5 µm, 4.6 mm × 20 mm, water) and eluted in mobile phase B (20 mmol/L ammonium formate (pH = 10) in 80% (v/v) acetonitrile) on BEH130C18 column (3.5 µm, 2.1 mm × 150 mm column, water). The flow rate of mobile phase B was 230 µL/min with a linear gradient as followed: (1) 0–9 min, 5%–15% B; (2) 9–30 min, 15%–50% B; (3) 30–41 min, 50%–90% B; (4) 41–60 min, 90% B. After elution, 27 fractions were collected, combined into 8 fractions with UV absorption at 214 nm, and then dried in a vacuum concentrator.

The dried fractions were dissolved in mobile phase C [0.1% (v/v) formic acid in water] and analyzed by nano-liquid chromatography-tandem mass spectrometry (LC-MS/MS) consisting of ultimate 3,000 coupled to Q-Exactive HF. The mobile phase D [0.1% (v/v) formic acid in acetonitrile] increased from 5% to 90% in 110 mins. The mass spectrometer was operated in the positive-ion mode at an ion transfer tube temperature of 300 °C with 2.2 kV positive-ion spray voltage. Orbitrap Velos was set up in Data-Dependent Acquisition (DDA) mode. The resolution of full-scan MS (350–2,000 m/z) in the Orbitrap analyzer was 60,000; the 20 most intense ions from the preceding MS were sequentially collected; the Normalized collision energy (NCE) was 27%; dynamic exclusion was set to an exclusion duration of 30 s and a repetition count of 1. The tandem mass spectra were searched against the human UniProt Non-redundant Reference database (2018.05) using Proteome Discoverer 2.2 software. As search parameters, a tolerance of 10 ppm was considered for precursor ions (MS search) and 0.02 Da for fragment ions (MS/MS search); the maximum number of missed cleavages was 2; carbamidomethylation of cysteine was set as a fixed modification; protein N-terminal oxidation of methionine was set as a variable modification. The search results are imported into skyline for data analysis of Data-Independent Acquisition (DIA).

The DIA was performed using the same liquid phase separation gradient as DDA; full scan MS spectra (350–1,200 m/z) is divided into 40 Da precursor isolation windows, and each parent window is sequentially selected, fragmented, and collected. All sub-ion information is used for quantification. The search results are imported into Skyline for data analysis. Protein abundances were calculated using the label-free quantitation algorithm (LFQ). LFQ Intensity was used for protein quantitation. The minimum ratio count of LFQ was set to 2. The false discovery rate (FDR) was set to 0.05.

Parallel Reaction Monitoring (PRM)

The samples were collected and pretreated in a similar way as Proteomics. The mobile phase D increased from 4% to 90% in 72 mins. The mass range of full-scan MS was 350–1,500 m/z. The resolution, ACG target, and Maximum IT were 30,000 at 200 m/z, 3e6, and 20 ms for the first ion MS, respectively. The ACG target was 1e5 and the maximum IT was 45 ms for the secondary ion MS. Isolation Windows is 1.0 m/z. Skyline software was used to analyze PRM data and differential expression protein data was analyzed with MSstats.

Statistical Analysis

Proteins with a P-value < 0.05 were considered differentially expressed. Differentially expressed proteins (DEPs) analysis of two groups (three biological replicates per group) was indicated with the absolute $\log_2$ (fold change of HQ/C) values. Gene Ontology (GO) enrichment analysis of DEPs was conducted using PANTHER (http://pantherdb.org/). The pathway analysis of DEPs was carried out using the Kyoto Encyclopedia of Genes and Genomes (KEGG) database (http://www.kegg.jp/). The protein-protein-interaction network was constructed using STRING (http://string-db.org/).

RESULTS

DEPs in HQ-induced K562 Cells

Our previous studies have demonstrated that hemin-induced erythroid differentiation is concentration-dependently and time-dependently inhibited by 0–80 µmol/L hydroquinone in K562 cells[7]. In the present study, the concentration of 40 µmol/L HQ was selected to correspond to no obvious cytotoxicity but markedly inhibiting erythroid differentiation in K562 cells when exposed for 72 h[7,11,16]. Label-free proteomic analysis was applied to analyze the differentially expressed proteins in HQ-induced K562 cells. The DEPs were assessed using a P-value less than 0.05. In Figure 1, the volcano plots summarized the fold change and significance for the protein levels in HQ-induced K562 cells. The results showed that 4,082 proteins were identified and 466 proteins were differentially expressed (P < 0.05) including 187 upregulated proteins and 279 downregulated proteins after HQ exposure. Moreover, there were 121 upregulated DEPs and 154 downregulated DEPs over 1.3-fold change after HQ exposure. Table 1 illustrated the top 10 upregulated DEPs and top 10 downregulated DEPs after HQ exposure for 72 h. ERCC1 increased to 9.62-fold of the control group after HQ exposure, which was the most upregulated DEP. IFITM1 decreased to 0.07-fold of the control group after HQ exposure, which was the most downregulated DEP.

DEPs in HQ-induced K562 Cells Validated with PRM

PRM is a targeted proteomics strategy that enables simultaneous monitoring of all products of a target peptide under conditions that offer high-resolution and high-mass accuracy[29]. Therefore, it has been widely applied to the validation of proteomics[30,31]. In our research, PRM quantitative analysis was performed. Based on the possible mechanisms suggested in the previous studies of HQ-induced hematotoxicity, including inhibition of erythroid differentiation, intervention of cell cycle and cell apoptosis, epigenetic changes (DNA methylation and histone modification) and signaling pathways, 16 upregulated DEPs and 17 downregulated DEPs were validated with PRM (Table 2). In terms of erythroid differentiation, CD44, ECM1, HBAT, ITA2B, CWC25, HBE, GATA1, HBAZ, and HBA were considerably upregulated, while HBG2 and CD11B were downregulated. In terms of cell cycle and cell apoptosis, CDK4 was upregulated, while IKKB and FADD were downregulated. In terms of DNA methylation and histone modification, TRAM1, NPL4, DNMT1 and HAT1 were significantly upregulated, while H2AZ, KDM1A, HDAC2, H2AY, H12, H31, and H32 were downregulated. In terms of signaling pathways, TGFB1 and BRAT1 were considerably up-regulated, while MTOR, SMAD3, STAT3, BCAT1, STA5B, and GSK3B were down-regulated. The changing trends of these DEPs were consistent with the analysis results of proteomic methods, confirming the reliability of the data.

GO Classification Analysis of DEPs

The HQ-upregulated DEPs were annotated with 820 GO annotations according to their biological processes, cellular components, and molecular functions. The top 30 enriched GO terms were shown in Figure 2. GO analysis of HQ-upregulated DEPs showed that the biological processes were enriched in neutrophil mediated immunity, granulocyte activation, proteasomal protein catabolic process, vacuolar transport, and aging; the cellular components were enriched in blood microparticle, vacuolar lumen, vesicle lumen, pigment granule and primary lysosome; the

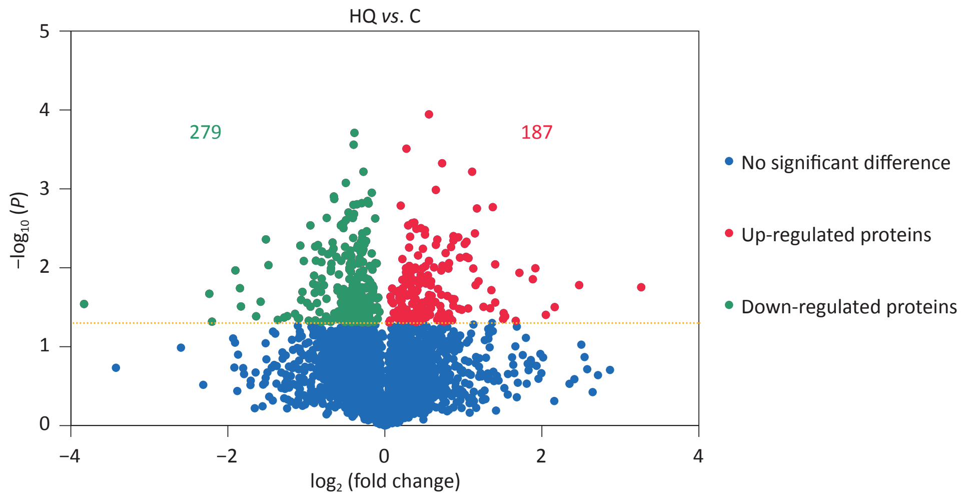

Figure 1. DEPs in HQ-induced K562 cells. K562 cells were induced with 0 and 40 μmol/L HQ for 72 h. The label-free proteomic assay was applied to analyze the DEPs in HQ-induced K562 cells. The volcano plot displays the differences in protein abundance detected between HQ and C groups. Each point represents one of the detected genes. Green points are downregulated DEPs, red points are upregulated DEPs and blue points are proteins without significant changes in HQ-induced K562 cells. Horizontal dotted lines indicate statistical thresholds for a *P*-value < 0.05 calculated using a two-tailed *t*-test. Data are representative of three independent experiments. HQ, hydroquinone-induced K562 cells; C, the control group; DEPs, differentially expressed proteins.

molecular functions were enriched in oxidoreductase activity acting on CH-OH group of donors, misfolded protein binding, ATPase binding, cell adhesion molecule binding and structural constituent of muscle (Figure 2A).

GO analysis of HQ-downregulated DEPs with 806 GO annotations showed that the biological processes were enriched in ribonucleotide metabolic process, cellular amino acid metabolic process, nucleoside monophosphate metabolic process, generation of precursor metabolites and energy and organic acid biosynthetic process; the cellular components were enriched in oxidoreductase complex, respiratory chain, mitochondrial protein complex, mitochondrial membrane part, and mitochondrial matrix; the molecular functions were enriched in electron transfer activity, cofactor binding, metal cluster binding, ligase activity and magnesium ion binding (Figure 2B).

Previous research has shown that HQ considerably inhibits hemin-induced erythroid differentiation in K562 cells[7,15,32,33]. Transcriptomic analysis and proteomic analysis contributed to high-throughput data for HQ-induced DEGs and DEPs in K562 cells. According to GO analysis results, there were a total of 23 DEGs and 5 DEPs in erythroid differentiation-related pathways (Table 3). In the positive regulation of erythrocyte differentiation term, *HSPA1A*, *HSPA1B*, *PRMT1,* and STAT1 were considerably upregulated, meanwhile, *ARNT*, *STAT3*, *NCKAP1L*, *STAT5B,* and *TRIM58* were downregulated. In the primitive erythrocyte differentiation term, *VEGFA* was significantly downregulated. In the enucleate erythrocyte development term, *MAEA* and *LYAR* were considerably upregulated, while *DMTN*, *CITED2*, *BCL6,* and LYAR were considerably downregulated. In the erythrocyte differentiation term, *KIT*, *EPAS1*, *CASP3,* and *HSPA9* were significantly upregulated, while *ALAS2*, *THRA*, *DNASE2*, *INHA,* and *SPI1* were significantly downregulated. In the erythrocyte maturation, HBAZ and G6PD were considerably upregulated, while ERCC2 was considerably downregulated. These results confirmed that HQ exposure might contribute to these genes and protein expression changes, affecting erythroid differentiation and maturation.

KEGG Pathway Analysis of DEPs

A Kyoto Encyclopedia of Genes and Genomes (KEGG) pathway-based functional enrichment

Table 1. Top 10 upregulated or downregulated DEPs in HQ-induced K562 cells

Accession	Protein name	Description	Log_2 (HQ/C)	*P*-value
P07992	ERCC1	ERCC excision repair 1, endonuclease non-catalytic subunit	3.27	0.02
P28799	GRN	granulin precursor	2.48	0.02
P13224	GP1BB	glycoprotein Ib platelet beta subunit	2.16	0.03
Q86YT6	MIB1	Mind bomb E3 ubiquitin protein ligase 1	2.05	0.04
Q96HR8	NAF1	nuclear assembly factor 1 ribonucleoprotein	1.92	0.01
Q16513	PKN2	protein kinase N2	1.88	0.01
P04004	VTN	vitronectin	1.71	0.01
Q96EK4	THAP11	THAP domain containing 11	1.67	0.05
Q04828	AKR1C1	Aldo-keto reductase family 1 member C1	1.53	0.04
P04003	C4BPA	complement component 4 binding protein alpha	1.51	0.04
Q16850	CYP51A1	cytochrome P450 family 51 subfamilies A member 1	−1.48	0.01
Q9UDW1	UQCR10	ubiquinol-cytochrome c reductase, complex III subunit X	−1.52	0.00
P09972	ALDOC	aldolase, fructose-bisphosphate C	−1.58	0.03
Q86UE8	TLK2	tousled like kinase 2	−1.64	0.04
Q6GMV3	PTRHD1	peptidyl-tRNA hydrolase domain containing 1	−1.83	0.03
Q16877	PFKFB4	6-phosphofructo-2-kinase/fructose-2,6-biphosphatase 4	−1.85	0.02
A8MPS7	YDJC	YdjC homolog (bacterial)	−1.90	0.01
P62736	ACTA2	actin, alpha 2, smooth muscle, aorta	−2.20	0.05
P16083	NQO2	NAD(P)H quinone dehydrogenase 2	−2.24	0.02
P13164	IFITM1	interferon induced transmembrane protein 1	−3.83	0.03

Note. HQ, hydroquinone; DEPs, differentially expressed proteins.

Table 2. Comparison of DEPs identified by PRO and PRM in HQ-induced K562 cells

Accession	Protein name	Description	PRO Log_2 (HQ/C)	PRM Log_2 (HQ/C)
Erythroid differentiation				
P16070	CD44	CD44 molecule (Indian blood group)	1.13	1.02
Q16610	ECM1	extracellular matrix protein 1	1.32	0.82
P09105	HBAT	hemoglobin subunit theta−1	0.71	0.79
P08514	ITA2B	integrin alpha-IIb	0.80	0.75
Q9NXE8	CWC25	CWC25 spliceosome associated protein homolog	0.63	0.65
P02100	HBE	hemoglobin subunit epsilon	0.48	0.60
P15976	GATA1	GATA binding protein 1; erythroid transcription factor	0.04	0.39
P02008	HBAZ	hemoglobin subunit zeta	0.27	0.36
P69905	HBA	hemoglobin subunit alpha	0.19	0.17
P69892	HBG2	hemoglobin subunit gamma-2	−0.58	−0.31
P21127	CD11B	cyclin-dependent kinase 11B	−0.18	−0.03
Cell cycle and cell apoptosis				
P11802	CDK4	cyclin-dependent kinase 4	0.63	1.08
O14920	IKKB	inhibitor of nuclear factor kappa-B kinase subunit beta	−0.36	−0.26
Q13158	FADD	FAS-associated death domain protein	−0.52	−0.32
DNA methylation and histone modification				
Q15629	TRAM1	translocation chain-associated membrane protein 1	0.36	0.62
Q8TAT6	NPL4	nuclear protein localization protein 4 homolog	0.24	0.47
P26358	DNMT1	DNA (cytosine-5)-methyltransferase 1	0.12	0.45
O14929	HAT1	histone acetyltransferase type B catalytic subunit	0.22	0.15
P0C0S5	H2AZ	H2A.Z variant histone	−0.72	−0.15
O60341	KDM1A	lysine-specific histone demethylase 1A	−0.43	−0.18
Q92769	HDAC2	histone deacetylase 2	−0.46	−0.20
O75367	H2AY	core histone macro-H2A.1	−0.25	−0.39
P16403	H12	histone H1.2	−0.46	−0.42
P68431	H31	histone H3.1	−0.89	−1.29
Q71DI3	H32	histone H3.2	−1.10	−1.75
Signaling pathways				
P01137	TGFB1	transforming growth factor beta−1 proprotein	0.23	0.73
P42345	MTOR	mechanistic target of rapamycin kinase; serine/threonine-protein kinase mTOR	−0.06	−0.31
P84022	SMAD3	mothers against decapentaplegic homolog 3	−0.43	−0.45
P40763	STAT3	signal transducer and activator of transcription 3	−0.14	−0.74
P54687	BCAT1	branched-chain-amino-acid aminotransferase 1, cytosolic	−1.08	−0.81
P51692	STA5B	signal transducer and activator of transcription 5B	−0.37	−1.12
P49841	GSK3B	glycogen synthase kinase-3 beta	−0.38	−1.15
Q6PJG6	BRAT1	BRCA1-associated ATM activator 1	0.44	0.35

***Note*.** DEPs, differentially expressed proteins; PRO, proteomics; PRM, parallel reaction monitoring; HQ, hydroquinone.

analysis was performed to determine the pathways associated with HQ-induced DEPs. The HQ-upregulated DEPs were annotated with 162 KEGG pathway map identifiers and the downregulated DEPs included 169 KEGG pathway identifiers. The top 14 enriched pathways of upregulated DEPs and the top 19 enriched pathways of downregulated DEPs were shown in Figure 3. KEGG pathway analysis demonstrated that HQ-upregulated DEPs were the most significantly enriched in the lysosome (hsa04142), followed by metabolic pathways (hsa01100), cell cycle (hsa04110), and cellular senescence (hsa04218) (Figure 3A). In addition, the HQ-downregulated DEPs were the most significantly enriched in metabolic pathways, followed by biosynthesis of amino acids (hsa01230), alzheimer disease (hsa05010), and thermogenesis (hsa04714) (Figure 3B).

Focusing on potential mechanisms of HQ-induced hematotoxicity revealed in previous research[14-16], there were 3, 6, 5, 4, and 4 DEPs annotated as the KEGG terms of cell cycle, cellular senescence, apoptosis, autophagy–animal, and necroptosis (Table 4). KEGG pathway analysis also showed the potentially related signaling pathways such as mTOR, p53, PI3K-Akt, MAPK, and AMPK signaling pathways (Supplementary Table S1 available in www.besjournal.com). Meanwhile, biological processes like ECM-receptor interaction, protein processing in the endoplasmic reticulum, hematopoietic cell lineage, and nucleotide excision repair were revealed (Supplementary Table S2, available in www.besjournal.com). Input DEPs of these pathways were illustrated in Supplementary Table S3, available in www.besjournal.com. These results suggested that HQ-induced hematotoxicity might be achieved by modulating the expression of these DEPs to affect related pathways.

The Networks of Protein Interactions in HQ-induced K562 Cells

Focusing on the erythroid differentiation-related pathways in the GO analysis results, the network of the 27 differently expressed proteins and differently expressed genes-related proteins were analyzed using STRING with a medium confidence score threshold of 0.4. After kmeans-clustering these proteins into four categories, an interactome network was built to find out protein-protein interaction and predict functional associations

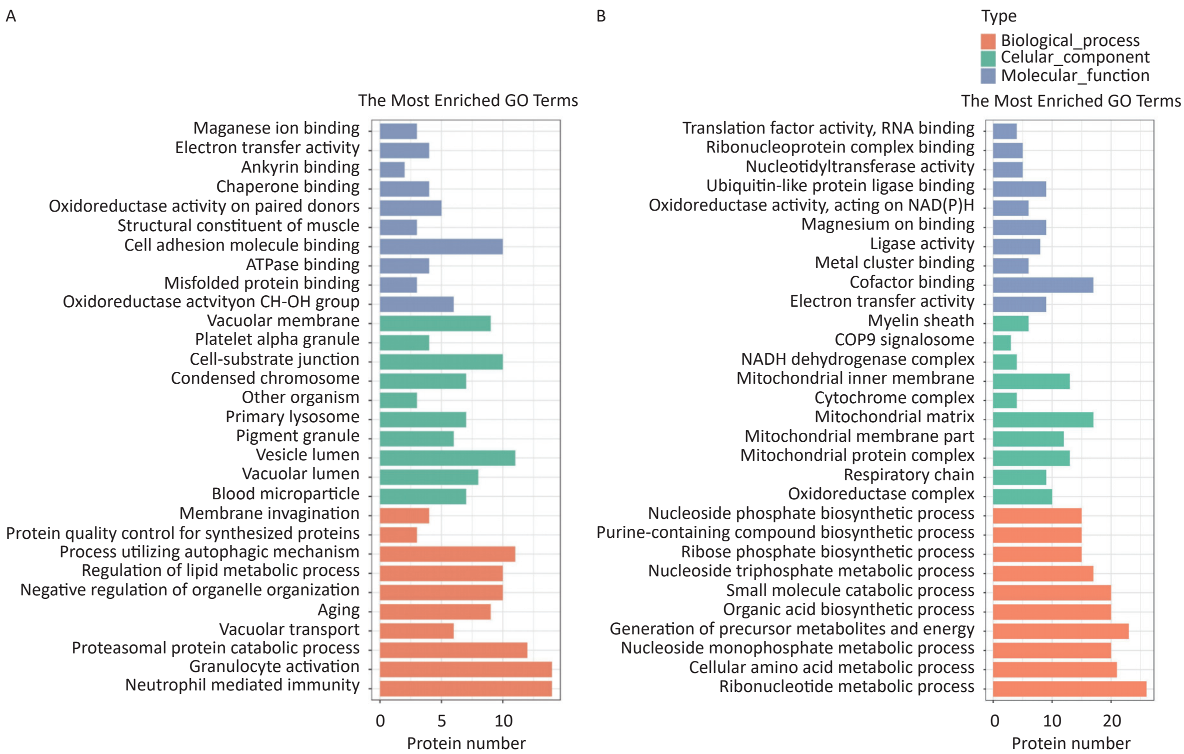

Figure 2. GO analysis of DEPs in HQ-induced K562 cells. (A) GO enrichment histogram of upregulated DEPs. (B) GO enrichment histogram of downregulated DEPs. GO, Gene Ontology; DEPs, differentially expressed proteins; HQ, hydroquinone.

among these significantly altered proteins (Figure 4). By analyzing the predicted protein networks, we determined six differentially expressed genes with the most interactions and they were STAT1, STAT3, CASP3, KIT, STAT5B, and VEGFA. STATs, named signal transducer and transcription activator, were identified as critical transcription factors in mediating virtually all cytokine-driven signaling and are thought to involve in various aspects of hematopoiesis, affecting cell proliferation, differentiation, and cell survival, meaning the dysregulation[34-36]. As shown in the networks, the

Table 3. GO analysis of DEGs and DEPs in erythrocyte differentiation-related pathways

Type	Name	Description	C	HQ	Log_2 (HQ/C)	*P*-value
GO:0045648 positive regulation of erythrocyte differentiation						
DEG	*HSPA1A*	Heat shock 70 kDa protein 1A	2380.07	3525.29	0.57	3.62×10^{-4}
DEG	*HSPA1B*	Heat shock 70 kDa protein 1B	1456.71	2047.15	0.49	2.13×10^{-4}
DEG	*PRMT1*	Protein arginine N-methyltransferase 1	7636.53	10241.65	0.42	2.76×10^{-3}
DEG	*ARNT*	Aryl hydrocarbon receptor nuclear translocator	1239.05	994.57	−0.32	4.42×10^{-2}
DEG	*STAT3*	Signal transducer and activator of transcription 3	7816.59	6107.88	−0.36	8.66×10^{-3}
DEG	*NCKAP1L*	Nck-associated protein 1-like	1588.34	1216.83	−0.38	7.45×10^{-3}
DEG	*STAT5B*	Signal transducer and activator of transcription 5B	7772.78	5916.55	−0.39	2.66×10^{-3}
DEG	*TRIM58*	E3 ubiquitin-protein ligase TRIM58	1235.03	853.23	−0.53	1.17×10^{-4}
DEP	STAT1	Signal transducer and activator of transcription 1	786.12	892.10	0.18	1.95×10^{-2}
GO:0060319 primitive erythrocyte differentiation						
DEG	*VEGFA*	Vascular endothelial growth factor A	6792.45	3236.41	−1.07	5.22×10^{-21}
GO:0048822 enucleate erythrocyte development						
DEG	*MAEA*	E3 ubiquitin-protein transferase MAEA	2162.55	2704.36	0.32	2.68×10^{-2}
DEG	*LYAR*	Cell growth-regulating nucleolar protein	753.96	1335.92	0.83	1.24×10^{-10}
DEG	*DMTN*	Dematin	5445.88	4230.23	−0.36	2.88×10^{-2}
DEG	*CITED2*	Cbp/p300-interacting transactivator 2	8346.68	5983.22	−0.48	1.55×10^{-4}
DEG	*BCL6*	B-cell lymphoma 6 protein	164.91	78.64	−1.07	5.25×10^{-7}
DEP	LYAR	Cell growth-regulating nucleolar protein	785.46	538.76	−0.54	3.79×10^{-2}
GO:0030218 erythrocyte differentiation						
DEG	*KIT*	Mast/stem cell growth factor receptor	205.96	370.51	0.85	2.74×10^{-7}
DEG	*EPAS1*	Endothelial PAS domain-containing protein 1	222.64	334.54	0.59	1.03×10^{-3}
DEG	*CASP3*	Caspase-3	378.35	560.44	0.57	4.95×10^{-2}
DEG	*HSPA9*	Stress-70 protein, mitochondrial	3536.24	4928.96	0.48	1.12×10^{-3}
DEG	*ALAS2*	5-aminolevulinate synthase, erythroid-specific, mitochondrial	2661.41	2008.50	−0.41	3.33×10^{-3}
DEG	*THRA*	Thyroid hormone receptor alpha	2398.39	1705.39	−0.49	2.22×10^{-4}
DEG	*DNASE2*	Deoxyribonuclease 2, lysosomal	377.89	259.76	−0.54	1.96×10^{-3}
DEG	*INHA*	Inhibin alpha chain	589.45	305.50	−0.95	2.95×10^{-10}
DEG	*SPI1*	Transcription factor PU.1	1375.22	661.69	−1.06	2.33×10^{-9}
GO:0043249 erythrocyte maturation						
DEP	HBAZ	Hemoglobin subunit zeta	1570.60	1893.60	0.27	1.14×10^{-2}
DEP	G6PD	Glucose-6-phosphate 1-dehydrogenase	1965.05	3121.64	0.67	4.39×10^{-3}
DEP	ERCC2	ERCC excision repair 2, TFIIH core complex helicase subunit	363.34	311.97	−0.22	1.42×10^{-3}

Note. GO, Gene Ontology; DEGs, differentially expressed genes; DEPs, differentially expressed proteins; HQ, hydroquinone-induced K562 cells; C, the controlgroup.

differential expressions of STAT1, STAT3, and STAT5B significantly impact the entire protein interaction network in HQ-induced K562 cells, which means the dysregulation of these proteins highly demands our attention.

DISCUSSION

Proteomics is the study of information about all the proteins expressed in an organism at a specific time and place, including the structure, location, and quantities[19,21,23]. Based on the bioinformatics database and bioinformatics analysis, we can further analyze the interaction relationship between DEPs and the signaling pathways and biological processes they affect. Compared with traditional genomics and transcriptomics analysis, proteomics can help us elucidate environmental pollutants' toxicological mechanisms more clearly and find the biomarkers more directly and precisely.

In this study, on comparing the HQ-induced and control K562 cells, 466 differentially expressed proteins were screened out, of which 187 proteins were upregulated and 279 were downregulated. In

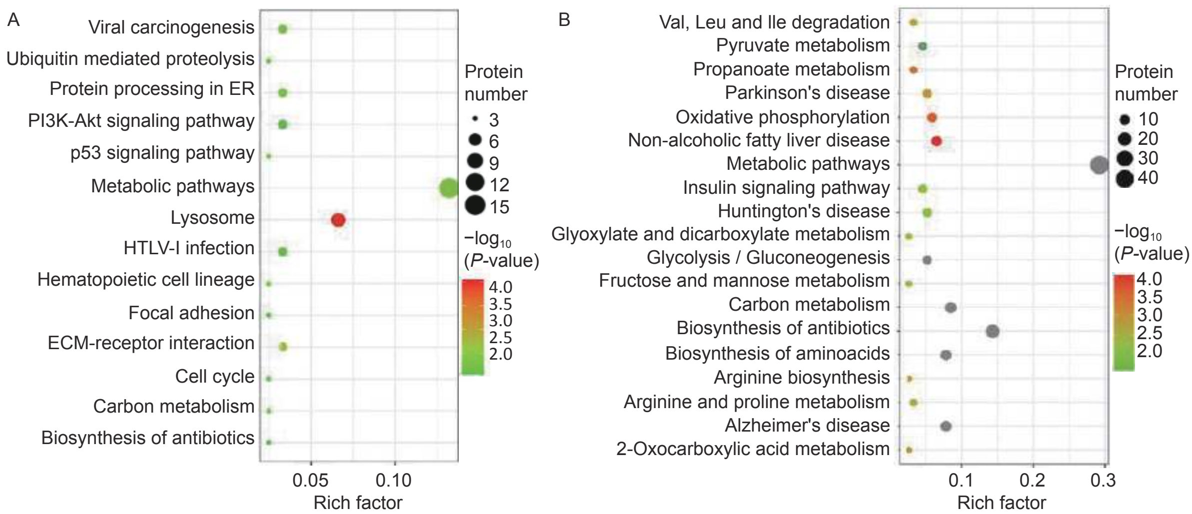

Figure 3. KEGG analysis for DEPs in HQ-induced K562 cells. (A) KEGG pathway enrichment analysis of upregulated DEPs. (B) KEGG pathway enrichment analysis of downregulated DEPs. Rich factor indicates the annotated DEPs number and whole background genes number ratio in the corresponding pathway. The size of each bubble corresponds to the number of annotated DEPs and the color gradient depicts the *P*-value of enrichment significance. KEGG, Kyoto Encyclopedia of Genes and Genomes; DEPs, differentially expressed proteins; HQ, hydroquinone.

Table 4. KEGG pathway analysis of DEPs in potential mechanisms of HQ-induced hematotoxicity

KEGG term	ID	Input number	Background number	Regulated	DEPs
Cellular senescence	hsa04218	5	160	up	SIRT1, NFATC2, CDK4, CAPN2, CHEK1
		1	160	down	RBBP4
Apoptosis	hsa04210	4	136	up	SPTAN1, CTSB, CTSD, CAPN2
		1	136	down	BID
Autophagy - animal	hsa04140	3	128	up	CTSB, CTSD, LAMP2
		1	128	down	RPS6KB2
Necroptosis	hsa04217	2	162	up	CHMP4A, CAPN2
		2	162	down	BID, GLUL
Cell cycle	hsa04110	3	124	up	BUB1B, CDK4, CHEK1

Note. KEGG, Kyoto Encyclopedia of Genes and Genomes; DEPs, differentially expressed proteins; HQ, hydroquinone.

our study, Excision repair cross-complementation group 1 (ERCC1), which forms heterodimers with the XPF endonuclease participating in nucleotide excision repair (NER) and genomic instability[37,38], was the most upregulated DEP. Myelodysplastic syndromes (MDS) are characterized by ineffective hemopoiesis leading to blood cytopenias[39]. Previous research implied that *ERCC1* promotes the aging process of erythroid cells and the induced *ERCC1* expression might reflect the premature aging of the MDS-derived erythroid precursors[40]. Our result enhanced this discovery and showed that the role of ERCC1 and DNA damage repair in HQ-induced hematotoxicity needs further study.

Following the GO classification of DEPs, the HQ upregulated and downregulated DEPs were annotated with GO annotations including neutrophil-mediated immunity, blood microparticle, ribonucleotide metabolic process, cellular amino acid metabolic process, electron transfer activity, and so on, which were associated with the occurrence of hematotoxicity. Since HQ-induced increase in intracellular ROS levels has been shown to be associated with erythroid differentiation and apoptosis in HL-60 promyelocytic leukemia cells, Jurkat T-lymphoblastic leukemia cells, JHP lymphoblastoid cells and K562 cells[12,15,16,41,42], we focused on the GO term of oxidative stress and

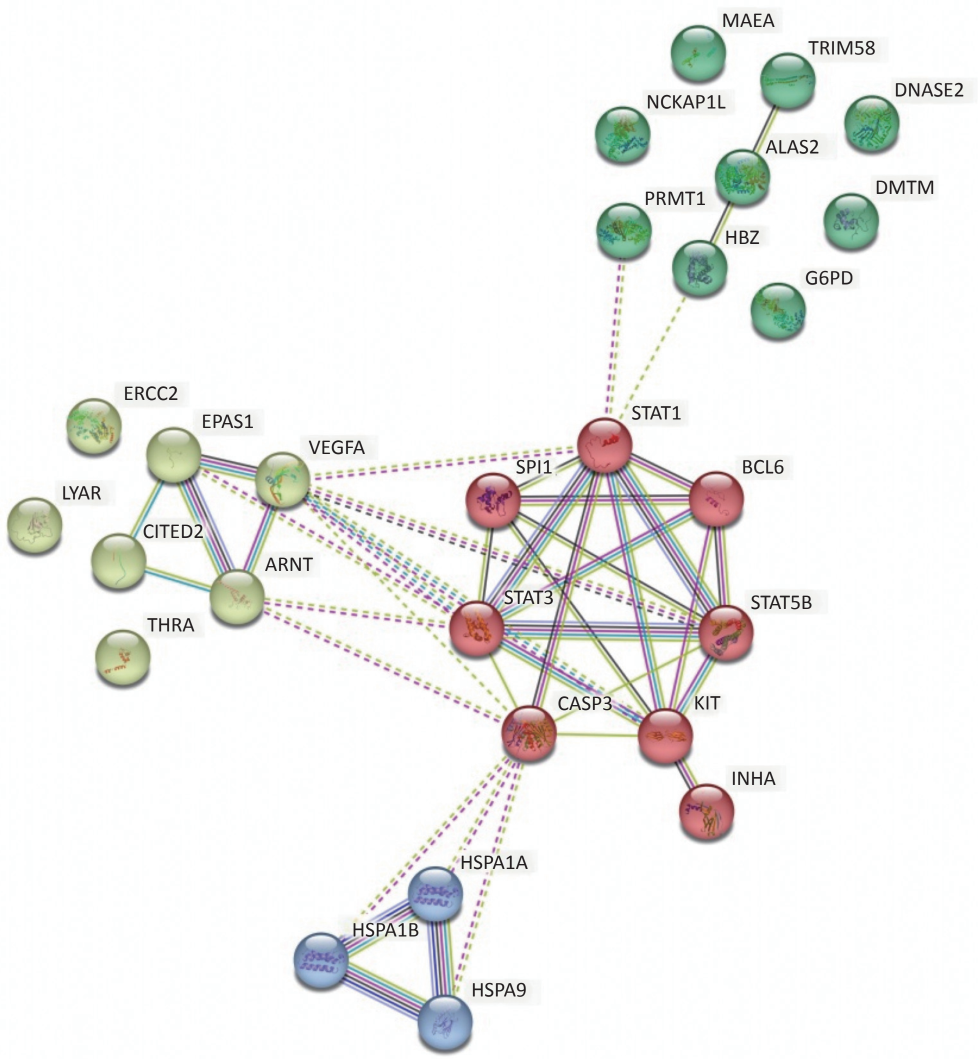

Figure 4. Predicted protein networks associated with the proteins upregulated or downregulated in HQ-exposed K562 cells. Cytoscape networks were constructed using 27 DEPs in erythroid differentiation-related pathways. Four bubbles in different colors indicate four clusters. DEPs, differentially expressed proteins; HQ, hydroquinone.

found there were 9 upregulated DEPs (ERCC1, AGAP3, SIRT1, G6PD, HSPB1, TOR1A, SOD2, CAPN2, NUDT1) and 7 downregulated DEPs (NDUFS8, PRDX2, NDUFS2, OXSR1, ADPRHL2, LDHA, PYCR1) in the response to oxidative stress term (GO:0006979), further indicating the essential roles of HQ-induced oxidative stress in K562 cells. Focusing on cell apoptotic, there were 5 upregulated DEPs (CD44, TAF9, SIRT1, HSPB1, SOD2) in the intrinsic apoptotic signaling pathway term (GO:0097193), 6 upregulated DEPs (CD44, TAF9, SIRT1, GSN, HSPB1, SOD2) in the regulation of apoptotic signaling pathway term (GO:2001233) and 4 downregulated DEPs (HK2, NDUFS1, BID, TIMM50) in the apoptotic mitochondrial changes term (GO:0008637). These results confirmed the HQ-induced apoptotic in K562 cells, human TK6 lymphoblastoid cells, human ARPE-19 retinal pigment epithelial cells, and so on described in previous literature[14-16,43,44], and revealed several potentially related downstream proteins.

Besides HQ-induced oxidative stress and apoptotic, we used KEGG pathway annotations and analysis to find that HQ-upregulated DEPs were the most significantly enriched in the lysosome, metabolic pathways, cell cycle, and cellular senescence. Previously, we found that HQ could induce a significant increase in cell population in the G_0/G_1 phase and a significant decrease in the S phase[16]. In recent years, it was reported that HQ increased the expressions of E4 transcription factor 1 (E4F1) mRNA and protein in HQ-induced malignant transformed TK6 cells (TK6-HT), and silencing E4F1 could block the G_2/M phase of the cell cycle, inhibiting the progress of cell cycle and cell growth[8]. The results of our research and analysis were consistent with these previous findings and elucidated the relevant pathways and specific mechanisms.

In addition, most DEPs were annotated as the metabolic pathways map identifier and played important roles in multiple signaling pathways and various biological processes. Among them, the upregulated CDK4 was annotated as an important participant in the p53 and PI3K-Akt signaling pathway, modulating cellular process and life course including cell cycle and cellular senescence. The uncontrolled proliferation of immature myeloid cells is often associated with cell cycle dysregulation, which might inhibit cell differentiation processes[45,46]. Cyclin-dependent kinases (CDKs) take an important part in cell cycle control, among which CDK4 mediates progression through the G_1 metaphase in conjunction with D-type cyclins[47,48]. Therefore, the mutation and abnormal expression of CDK4 have important effects on hematotoxicity and disease progression, meanwhile, researchers are committed to developing CDK4-targeted treatment strategies[47,49].

To further explore the mechanism of HQ-induced hematotoxicity, we focused on the 23 DEGs and 5 DEPs in erythroid differentiation-related pathways in the GO analysis results and constructed the network of protein interactions in K562 cells. We determined 6 DEPs with the most interactions, which were STAT1, STAT3, CASP3, KIT, STAT5B, and VEGFA, and the differential expressions of STAT1, STAT3, and STAT5B make a central impact. Hematopoietic development is highly dependent on cytokine/receptor-initiated signaling pathways[50]. The activation of STATs mediates cellular signal transduction initiated by cytokines and growth factors with cognate receptors, especially the Janus kinase (JAK)-STAT pathway plays important roles in hematopoiesis by affecting the production of mature hematopoietic cells *via* effects on cellular proliferation, survival, and lineage-specific differentiation[51-53]. STAT1 is a pivotal downstream mediator of interferon (IFN) signaling required for IFN-induced hematopoietic stem cells (HSCs) proliferation[54]. The phosphorylated STAT1 enhanced secretion of TRAIL to induce cell apoptotic in KMS-20 cells through JAK/STAT pathway activation[55], while recent research showed that STAT1 is also critical for hematopoietic stem and progenitor cells (HSPCs) homeostasis maintenance by regulating HSCs self-renewal and intrinsic functions[56]. STAT3 is also an important gene expression regulator in the cell cycle, antiapoptosis, angiogenesis, and invasion/ migration[52]. It not only promotes the development of B and T cell subsets but also regulates neutrophil numbers and hematopoietic stem cell self-renewal[57]. Thus STAT3 has been identified as a therapeutic target for a wide range of diseases[52,57,58]. In addition to STAT1 and STAT3, STAT5 also regulates cell proliferation, differentiation, and survival critically[59]. STAT5 deletion can cause significant development defects in both lymphoid and myeloid lineages, and STAT5 is indispensable at later stages for normal granulopoiesis by mechanisms like regulating proliferation and survival genes to direct Granulocyte macrophage-colony stimulating factor (GM-CSF) signaling[60,61]. Therefore, HQ regulates the expression of these DEGs and DEPs associated with hematopoietic cell development, maturation, and differentiation to affect the production of mature erythrocytes and other blood cells with normal physiological functions. Further elucidation of the functions, interactions, and signal transduction involved in them will help us understand HQ-induced hematotoxicity.

CONCLUSION

In summary, this study demonstrated that the benzene metabolite HQ induced various protein expression changes in K562 cells, directly affecting intracellular signaling pathways and metabolic activities and consequently leading to hematotoxicity. Our study showed that STATs may be potential biomarkers of HQ-induced hematotoxicity and deserve attention. The DEP-associated changes shown in this article will shed light on future in-depth studies of the underlying mechanisms of HQ-induced hematotoxicity. Focusing on critical DEPs identified, more research can be carried out to find the intrinsic relationship between DEPs and other HQ-induced changes, such as DNA methylation, ROS increase, miRNAs expression changes, and histone modification. Further research and validation at the molecular level are needed to investigate these DEPs and their associated potential mechanisms. Coupled with cross-omics analysis and animal model studies, the mechanism of HQ-induced hematotoxicity will be presented more clearly and completely.

ACKNOWLEDGMENTS

Not applicable.

COMPETING INTERESTS

The authors declare that they have no conflict of interest.

AUTHORS' CONTRIBUTIONS

The manuscript was written by JIN Yi Shan and YI Zong Chun. The acquisition, analysis, and interpretation of data were done by JIN Yi Shan, YI Zong Chun, ZHANG Yu Jing, and YU Chun Hong. RONG Long and YU Chun Hong revised the article and gave final approval for the version to be submitted. All authors read and discussed the final draft of the manuscript.

Received: July 13, 2023;
Accepted: December 4, 2023

REFERENCES

1. Mehlman MA. Dangerous and cancer-causing properties of products and chemicals in the oil refining and petrochemical industries. Part XXX: Causal relationship between chronic myelogenous leukemia and benzene-containing solvents. Ann N Y Acad Sci, 2006; 1076, 110−9.
2. Spatari G, Allegra A, Carrieri M, et al. Epigenetic effects of benzene in hematologic neoplasms: the altered gene expression. Cancers (Basel), 2021; 13, 2392.
3. McDonald TA, Holland NT, Skibola C, et al. Hypothesis: phenol and hydroquinone derived mainly from diet and gastrointestinal flora activity are causal factors in leukemia. Leukemia, 2001; 15, 10−20.
4. Zhang LP, McHale CM, Rothman N, et al. Systems biology of human benzene exposure. Chem Biol Interact, 2010; 184, 86−93.
5. Sarma SN, Kim YJ, Ryu JC. Differential gene expression profiles of human leukemia cell lines exposed to benzene and its metabolites. Environ Toxicol Pharmacol, 2011; 32, 285−95.
6. Rubio V, Zhang JW, Valverde M, et al. Essential role of Nrf2 in protection against hydroquinone- and benzoquinone-induced cytotoxicity. Toxicol in Vitro, 2011; 25, 521−9.
7. Wu XR, Xue M, Li XF, et al. Phenolic metabolites of benzene inhibited the erythroid differentiation of K562 cells. Toxicol Lett, 2011; 203, 190−9.
8. Tan Q, Li JY, Peng JM, et al. E4F1 silencing inhibits cell growth through cell -cycle arrest in malignant transformed cells induced by hydroquinone. J Biochem Mol Toxicol, 2019; 33, e22269.
9. Liang BX, Chen YC, Yuan WX, et al. Down-regulation of miRNA-451a and miRNA-486-5p involved in benzene-induced inhibition on erythroid cell differentiation in vitro and in vivo. Arch. Toxicol, 2018; 92, 259−72.
10. Li Y, Wu XR, Li XF, et al. Changes in DNA methylation of erythroid-specific genes in K562 cells exposed to phenol and hydroquinone. Toxicology, 2013; 312, 108−14.
11. Tang KY, Yu CH, Jiang L, et al. Long-term exposure of K562 cells to benzene metabolites inhibited erythroid differentiation and elevated methylation in erythroid specific genes. Toxicol Res, 2016; 5, 1284−97.
12. Ishihama M, Toyooka T, Ibuki Y. Generation of phosphorylated histone H2AX by benzene metabolites. Toxicol in Vitro, 2008; 22, 1861−1868.
13. Zeng MJ, Chen SP, Zhang K, et al. Epigenetic changes involved in hydroquinone-induced mutations. Toxin Reviews, 2021; 40, 527−34.
14. Chen YT, Chen SY, Liang HR, et al. Bcl-2 protects TK6 cells against hydroquinone-induced apoptosis through PARP-1 cytoplasm translocation and stabilizing mitochondrial membrane potential. Environ Mol Mutagen, 2018; 59, 49−59.
15. Yu CH, Suriguga, Li Y, et al. The Role of ROS in Hydroquinone-induced Inhibition of K562 Cell Erythroid Differentiation. Biomed Environ Sci, 2014; 27, 212−4.
16. Wang Y, Zhang GY, Han QL, et al. Phenolic metabolites of benzene induced caspase-dependent cytotoxicities to K562 cells accompanied with decrease in cell surface sialic acids. Environ Toxicol, 2014; 29, 1437−51.
17. Mozzoni P, Poli D, Pinelli S, et al. Benzene exposure and MicroRNAs expression: in vitro, in vivo and human findings. Int J Environ Res Public Health, 2023; 20, 1920.
18. Yu CH, Yang SQ, Li L, et al. Identification of potential pathways and microRNA-mRNA networks associated with benzene metabolite hydroquinone-induced hematotoxicity in human leukemia K562 cells. BMC Pharmacol Toxicol, 2022; 23, 20.

19. Yipel M, İlhan A. Potentiation of toxicology with proteomics: toxicoproteomics. Int J Vet Anim Res, 2022; 5, 36−9.
20. Hansen MS, Rasmussen M, Grauslund J, et al. Proteomic analysis of vitreous humour of eyes with diabetic macular oedema: a systematic review. Acta Ophthalmol, 2022; 100, e1043−51.
21. Hanash S. Disease proteomics. Nature, 2003; 422, 226−32.
22. Dowling VA, Sheehan D. Proteomics as a route to identification of toxicity targets in environmental toxicology. Proteomics, 2006; 6, 5597−604.
23. Hall DR, Peng H. Characterizing physical protein targets of chemical contaminants with chemical proteomics: Is it time to fill a crucial environmental toxicology knowledge gap? Comparat Biochem Physiol Part D Genom Proteom, 2020; 34, 100655.
24. Hu JJ, Ma HM, Zhang WB, et al. Effects of benzene and its metabolites on global DNA methylation in human normal hepatic l02 cells: effects of benzene and its metabolites on global DNA methylation. Environ Toxicol, 2014; 29, 108−16.
25. Guo JM, Miao Y, Xiao BX, et al. Differential expression of microRNA species in human gastric cancer versus non-tumorous tissues. J Gastroenterol Hepatol, 2009; 24, 652−7.
26. McHale CM, Zhang LP, Lan Q, et al. Global gene expression profiling of a population exposed to a range of benzene levels. Environ Health Perspect, 2011; 119, 628−40.
27. Lozzio CB, Lozzio BB. Human chronic Myelogenous leukemia cell-line with positive Philadelphia chromosome. Blood, 1975; 45, 321−34.
28. Andersson LC, Jokinen M, Gahmberg CG. Induction of erythroid differentiation in the human leukaemia cell line K562. Nature, 1979; 278, 364−5.
29. Peterson AC, Russell JD, Bailey DJ, et al. Parallel reaction monitoring for high resolution and high mass accuracy quantitative, targeted proteomics. Mol Cell Proteom, 2012; 11, 1475−88.
30. Van Der Ende EL, Meeter LH, Stingl C, et al. Novel CSF biomarkers in genetic frontotemporal dementia identified by proteomics. Ann Clin Transl Neurol, 2019; 6, 698−707.
31. Di B, Jia HL, Luo OJ, et al. Identification and validation of predictive factors for progression to severe COVID-19 pneumonia by proteomics. Sig Transduct Target Ther, 2020; 5, 217.
32. Ma XJ, Zhang X, Luo J, et al. MiR-486-5p-directed *MAGI1/Rap1/RASSF5* signaling pathway contributes to hydroquinone-induced inhibition of erythroid differentiation in K562 cells. Toxicol in Vitro, 2020; 66, 104830.
33. Yu CH, Yang SQ, Zhang YJ, et al. The role of GATA switch in benzene metabolite hydroquinone inhibiting erythroid differentiation in K562 cells. Arch Toxicol, 2023; 97, 2169−81.
34. Bromberg J, Darnell JE. The role of STATs in transcriptional control and their impact on cellular function. Oncogene, 2000; 19, 2468−73.
35. Coffer PJ, Koenderman L, de Groot RP. The role of STATs in myeloid differentiation and leukemia. Oncogene, 2000; 19, 2511−22.
36. Fasouli ES, Katsantoni E. JAK-STAT in early hematopoiesis and leukemia. Front Cell Dev Biol, 2021; 9, 669363.
37. Faridounnia M, Folkers GE, Boelens R. Function and interactions of ERCC1-XPF in DNA damage response. Molecules, 2018; 23, 3205.
38. Wang SL, Zhao H, Zhou B, et al. Polymorphisms in ERCC1 and susceptibility to childhood acute lymphoblastic leukemia in a Chinese population. Leuk Res, 2006; 30, 1341−5.
39. Adès L, Itzykson R, Fenaux P. Myelodysplastic syndromes. Lancet, 2014; 383, 2239−52.
40. Huang HJ, Xu CL, Gao J, et al. Severe ineffective erythropoiesis discriminates prognosis in myelodysplastic syndromes: analysis based on 776 patients from a single centre. Blood Cancer J, 2020; 10, 83.
41. Kim YJ, Woo HD, Kim BM, et al. Risk assessment of hydroquinone: differential responses of cell growth and lethality correlated to hydroquinone concentration. J Toxicol Environ Health, Part A, 2009; 72, 1272−8.
42. Yang XH, Li C, Yu GC, et al. Ligand-independent activation of AhR by hydroquinone mediates benzene-induced hematopoietic toxicity. Chem Biol Interact, 2022; 355, 109845.
43. Song SM, Cerella C, Orlikova-Boyer B, et al. Hydroquinone-derivatives induce cell death in chronic Myelogenous leukemia. Proceedings, 2019; 11, 28.
44. Sun ZW, Chen C, Wang L, et al. S-allyl cysteine protects retinal pigment epithelium cells from hydroquinone-induced apoptosis through mitigating cellular response to oxidative stress. Eur Rev Med Pharmacol Sci, 2020; 24, 2120−8.
45. Hanahan D, Weinberg RA. Hallmarks of cancer: the next generation. Cell, 2011; 144, 646−74.
46. Dewi R, Hamid ZA, Rajab N, et al. Genetic, epigenetic, and lineage-directed mechanisms in benzene-induced malignancies and hematotoxicity targeting hematopoietic stem cells niche. Hum Exp Toxicol, 2020; 39, 577−95.
47. Baker SJ, Reddy EP. CDK4: A key player in the cell cycle, development, and cancer. Genes Cancer, 2012; 3, 658−69.
48. Piezzo M, Cocco S, Caputo R, et al. Targeting cell cycle in breast cancer: CDK4/6 inhibitors. Int J Mol Sci, 2020; 21, 6479.
49. Schneeweiss-Gleixner M, Byrgazov K, Stefanzl G, et al. CDK4/CDK6 inhibition as a novel strategy to suppress the growth and survival of *BCR-ABL1*^{T315I}+ clones in TKI-resistant CML. EBioMedicine, 2019; 50, 111−21.
50. Bunting KD. STAT5 signaling in normal and pathologic hematopoiesis. Front Biosci, 2007; 12, 2807−20.
51. Darnell JE. STATs and gene regulation. Science, 1997; 277, 1630−5.
52. Furtek SL, Backos DS, Matheson CJ, et al. Strategies and approaches of targeting STAT3 for cancer treatment. ACS Chem Biol, 2016; 11, 308−18.
53. Dorritie KA, McCubrey JA, Johnson DE. STAT transcription factors in hematopoiesis and leukemogenesis: opportunities for therapeutic intervention. Leukemia, 2014; 28, 248−57.
54. Darnell JE Jr, Kerr IM, Stark GR. Jak-STAT pathways and transcriptional activation in response to IFNs and other extracellular signaling proteins. Science, 1994; 264, 1415−21.
55. Miura Y, Tsujioka T, Nishimura Y, et al. TRAIL expression up-regulated by interferon-*γ* *via* phosphorylation of STAT1 induces myeloma cell death. Anticancer Res, 2006; 26, 4115−24.
56. Li J, Williams MJ, Park HJ, et al. STAT1 is essential for HSC function and maintains MHCII^{hi} stem cells that resist myeloablation and neoplastic expansion. Blood, 2022; 140, 1592−606.
57. Hankey PA. Regulation of hematopoietic cell development and function by Stat3. Front Biosci, 2009; 14, 5273−90.
58. Chong PSY, Chng WJ, De Mel S. STAT3: A promising therapeutic target in multiple myeloma. Cancers (Basel), 2019; 11, 731.
59. Rani A, Murphy JJ. STAT5 in Cancer and Immunity. J Interferon Cytokine Res, 2016; 36, 226−37.
60. Kimura A, Rieger MA, Simone JM, et al. The transcription factors STAT5A/B regulate GM-CSF-mediated granulopoiesis. Blood, 2009; 114, 4721−8.
61. Wang ZQ, Bunting KD. STAT5 in hematopoietic stem cell biology and transplantation. JAK-STAT, 2013; 2, e27159.